Electrical Power and Energy Systems 43 (2012) 859–867

Contents lists available at SciVerse ScienceDirect

Electrical Power and Energy Systems

journal homepage: www.elsevier.com/locate/ijepes

Model predictive based load frequency control_design concerning wind turbines

Tarek Hassan Mohamed [b,*], Jorge Morel [c], Hassan Bevrani [a], Takashi Hiyama [c]

[a] Dept. of Electrical & Computer Engineering, University of Kurdistan, Sanandaj, Iran
[b] Faculty of Energy, Aswan University, Egypt
[c] Dept. of Electrical & Computer Engineering, Kumamoto University, Kumamoto, Japan

ARTICLE INFO

Article history:
Received 28 October 2011
Received in revised form 18 April 2012
Accepted 5 June 2012

Keywords:
Load frequency control
Integral control
Model predictive control
Wind turbine

ABSTRACT

This paper presents a load frequency control (LFC) design using the model predictive control (MPC) technique in a multi-area power system in the presence of wind turbines. In the studied system, each local area controller is designed independently such that stability of the overall closed loop system is guaranteed. A frequency response model of multi-area power system including wind turbines is introduced. A physical constraints of the governors and turbines are considered in the model. The model was employed in the MPC structures. Digital simulations for a two area power system are provided to validate the effectiveness of the proposed scheme. The results show that, with the proposed MPC technique, the overall closed loop system performance demonstrated robustness in the face of uncertainties due to governors and turbines parameters variation and load disturbances. Also, it was denoted that wind turbine has a positive effect on the total response of the system. A performance comparison between the proposed controller with and without the participation of the wind turbines and a classical integral control scheme is carried out for confirming the superiority of the proposed MPC technique in the presence of the participation of the wind turbines.

© 2012 Published by Elsevier Ltd.

Author Personal Copy

1. Introduction

In fact, the LFC becomes an important function of power system operation where the main objective is to regulate the output power of each generator at prescribed levels while keeping the frequency fluctuations within pre-specified limits. Different types of controllers have been proposed in literature for the load frequency control design. The proportional integral PI controller, is widely employed in the LFC application [1]. But this type is considered as a fixed parameters controller which designed at nominal operating points and may no longer be suitable in all operating conditions. For this reason, adaptive gain scheduling approaches have been proposed for LFC synthesis [2–4].

Robust adaptive control schemes have been developed to deal with changes in system parameters. Fuzzy logic controllers have been used in many reports for LFC design in a two area power system [5], with and without nonlinearities. The applications of artificial neural network, genetic algorithms, and optimal control to LFC have been reported in [6,7]. In their findings it is observed that the transient response is oscillatory and it seems some other elegant techniques are needed to achieve a desirable performance. On the other hand, the MPC appears to be an efficient strategy to control many applications in industry, it has many advantages such as fast response, robustness against load disturbance and parameters uncertainty.

Its straightforward design procedure is considered as a major advantage of the MPC. Given a model of the system, only an objective function incorporating the control objectives needs to be set up. Additional physical constraints can be easily dealt with by adding them as inequality constraints, whereas soft constraints can be accounted for in the objective function using large penalties. Moreover, the MPC is well adapted to different physical setups and it allows for a unified approach [8–10].

Recently, a few attempts studied the idea of wind turbines in the issue of LFC. Variable speed wind turbines (VSWTs), the most utilize type of modern WTs, is partially or totally decoupled from the power network due to the power electronic converters limiting their capacity to provide primary frequency support to the network in case of disturbances. The inertial response of WTs is discussed in detail in [11,12].

A detailed background of frequency responses, including primary and secondary responses, are given in [11]. A detailed comparison is made about fixed-speed wind turbines (FSWTs) and doubly fed induction generator (DFIG) type wind turbines (WTs) through detailed simulations, the potential of FSWTs to contribute to the frequency response. On the other hand, these simulations also show that the DFIG-based WTs have negligible contribution

* Corresponding author.
E-mail addresses: tarekfoe@yahoo.com (T.H. Mohamed), bervrani@uok.ac.ir (H. Bevrani).

0142-0615/$ - see front matter © 2012 Published by Elsevier Ltd.
http://dx.doi.org/10.1016/j.ijepes.2012.06.032

to frequency responses and, hence it sounds that an additional control loop is necessary.

In [12], it is reported that full converter (FC) type WTs are completely decoupled from the power grid and no contribution is given to the frequency regulation. In addition, it is pointed out that the DFIG-type WTs have some small contribution to the power network.

In [13], and [15], fast response and robustness against parameter uncertainties and load changes can be obtained using MPC controller for both single and multi-area load frequency control application respectively, but without the participation of WTs.

While in [16], an attempt of study the effect of merging the wind turbines in the power system controlled by model predictive load frequency control method, a positive effect on the system response could be noted, but that only for a single area.

This paper studies the effect of merging the wind turbines on the system frequency response of multi area power system. In this paper, each local area includes an aggregated wind turbine model (which consists of 200 wind turbine units) beside the main generation unit. The MPC technique law produces its optimal output derived from a quadratic cost function minimization based on the dynamic model of the single area power system.The technique calculates the optimal control signal while respecting the given constrains over the output frequency deviation and the load change. The effects of the physical constraints such as generation rate constraint (GRC) and speed governor dead band [1] are considered. The power system with the proposed MPC technique has been tested through the effect of uncertainties due to governor and turbine parameters variation and load disturbance using computer simulation. A comparison has been made between the MPC (with and without wind turbine participation) and the traditional integral controller confirming the superiority of the proposed MPC technique and showing the positive effect of the WT participation on the total system performance. Also, the simulation results proved that the proposed controller can be successfully applied to the application of power system load frequency control.

The rest of the paper is organized as follows: A simplified wind turbine model is presented in Section 2. The description of the dynamics of the power system is given in Section 3. General consideration about MPC and its cost function are presented in Section 4. The implementation scheme of a multi area power system together with the MPC technique is described in Section 5. Simulation results and general remarks are presented in Section 6. Finally, the paper is concluded in Section 7.

2. Simplified wind turbine model for frequency studies

Fig. 1 shows a simplified model of DFIG based wind turbine for frequency response [14]. This simplified model can be described by the following equations:

$$\dot{i_{qr}} = -\left(\frac{1}{T_1}\right) i_{qr} + \left(\frac{X_2}{T_1}\right) V_{qr} \tag{1}$$

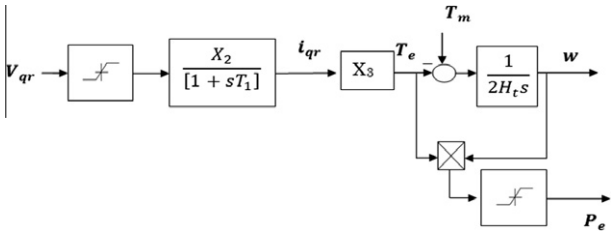

Fig. 1. Simplified model of DFIG based wind turbine.

Table 1
Parameters for Fig. 1 [14].

X_2	X_3	T_1
$\frac{1}{R_r}$	$\frac{L_m}{L_{ss}}$	$\frac{L_0}{w_s R_s}$

$$\dot{w} = -\left(\frac{X_3}{2H_t}\right) i_{qr} + \left(\frac{1}{2H_t}\right) T_m \tag{2}$$

$$P_e = wX_3 i_{qr} \tag{3}$$

and for linearization, Eq. (3) can be rewritten as:

$$P_e = w_{opt} X_3 i_{qr} \tag{4}$$

and

$$T_e = i_{qs} = -\frac{L_m}{L_{SS}} i_{qr} \tag{5}$$

where the parameters are defined as follows: w_{opt} is the operating point of the rotational speed, T_e the electromagnetic torque, T_m the mechanical power change, w the rotational speed, P_e the active power of wind turbine, i_{qr} the q-axis component of the rotor current, V_{qr} the q-axis component of the rotor voltage, H_t the equivalent inertia constant of wind turbine.

Table 1 shows the detailed expressions of the main parameters utilized for the simplified model of Fig. 1.where

$$L_0 = \left[L_{rr} + \frac{L_m^2}{L_{ss}}\right],\ L_{ss} = L_s + L_m,\ L_{rr} = L_{rs} + L_m$$

and L_m is the magnetizing inductance, R_r and R_s the rotor and stator resistances, respectively, L_r and L_s the rotor and stator leakage inductances, respectively, L_{rr} and L_{ss} the rotor and stator self-inductances, respectively, w_s is the synchronous speed.

3. System dynamics

A multi-area power system comprises areas that are interconnected by tie-lines. The trend of frequency measured in each control area is an indicator of the trend of the mismatch power in the interconnection and not in the control area alone. The LFC system in each control area of an interconnected (multi-area) power system should control the interchange power with the other control areas as well as its local frequency. Therefore, the dynamic LFC system model must take into account the tie-line power signal. For this purpose, consider Fig. 2, which shows a power system with N-control areas [1].

In this section, a frequency response model for any area-i of N power system control areas with an aggregated generator unit in each area is described [1].

The overall generator–load dynamic relationship between the incremental mismatch power ($\Delta P_{mi} - \Delta P_{Li}$) and the frequency deviation (Δf_i) can be express

$$\Delta \dot{f}_i = \left(\frac{1}{2H_i}\right)\Delta P_{mi} - \left(\frac{1}{2H_i}\right)\Delta P_{Li} - \left(\frac{D_i}{2H_i}\right)\Delta f_i - \left(\frac{1}{2H_i}\right)\Delta P_{tie,i} \tag{6}$$

the dynamic of the governor can be expressed as:

$$\Delta \dot{P}_{mi} = \left(\frac{1}{T_{ti}}\right)\Delta P_{gi} - \left(\frac{1}{T_{ti}}\right)\Delta P_{mi} \tag{7}$$

the dynamic of the turbine can be expressed as:

$$\Delta \dot{P}_{gi} = \left(\frac{1}{T_{gi}}\right)\Delta P_{ci} - \left(\frac{1}{R_i T_{gi}}\right)\Delta f_i - \left(\frac{1}{T_{gi}}\right)\Delta P_{gi} \tag{8}$$

Author Personal Copy

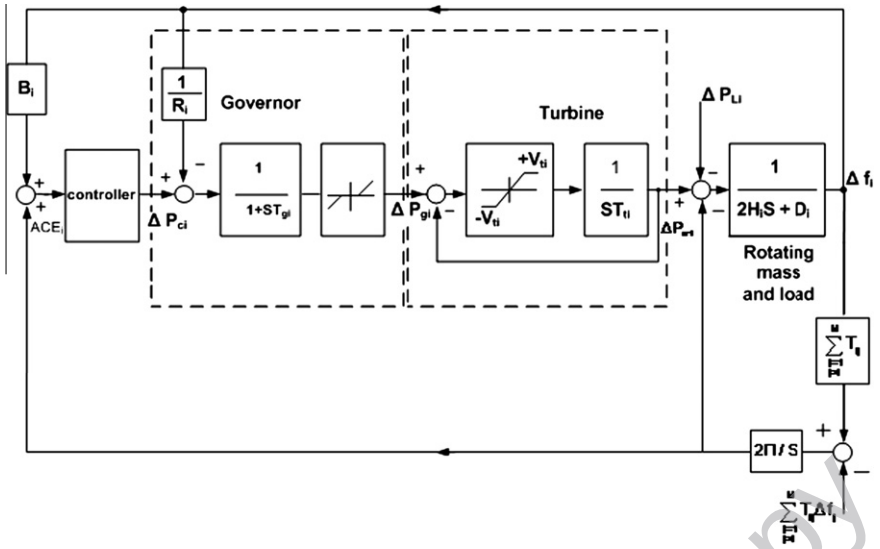

Fig. 2. Dynamic model of a control area in an interconnected environment.

the total tie-line power change between area-i and the other areas can be calculated as:

$$\Delta\dot{P}_{tie,i} = 2\pi\left[\sum_{\substack{j=1\\ j\neq i}}^{N} T_{ij}\Delta f_i - \sum_{\substack{j=1\\ j\neq i}}^{N} T_{ij}\Delta f_j\right] \tag{9}$$

In a multi-area power system, in addition to regulating area frequency, the supplementary control should maintain the net interchange power with neighbouring areas at scheduled values. This is generally accomplished by adding a tie-line flow deviation to the frequency deviation in the supplementary feedback loop. A suitable linear combination of frequency and tie-line power changes for area i, is known as the area control error (ACE),

$$ACE_i = \Delta P_{tie,i} + B_i\Delta f_i \tag{10}$$

Eqs. (6)–(9) in additionally to Eqs. (1) and (2) represent the frequency response model for N power system control areas with one generator unit and wind turbine unit in each area and can be combined in the following state space model:

where P_{gi} is the governor output change of area i. P_{mi} the mechanical power change of area i. f_i the frequency deviation of area i. P_{Li} the load change of area i. P_{ci} the supplementary control action of area i. y_i the system output of area i. H_i the equivalent inertia constant of area i. D_i the equivalent damping coefficient of area i. R_i the speed droop characteristic of area i. T_{gi}, T_{ti} the governor and turbine time constants of area i. ACE_i the control error of area i. B_i the a frequency bias factor of area i. T_{ij} the tie-line synchronizing coefficient with area j. $\Delta P_{tie,i}$ the total tie-line power change between area i and the other areas. Δv_i the control area interface, $\Delta v_i = \sum_{\substack{j=1\\ j\neq i}}^{N} T_{ij}\Delta f_j$

This state space model will be applied to the controller of the wind turbine unit, while the state space model used in the power system area controller will not include the dynamics of the wind turbine, and can be expressed as:

$$\left\{\begin{array}{l} \begin{bmatrix} \Delta\dot{P}_{gi}\\ \Delta\dot{P}_{mi}\\ \Delta\dot{f}_i\\ \Delta\dot{P}_{tie,i} \end{bmatrix} = \begin{bmatrix} -\frac{1}{T_{gi}} & 0 & -\frac{1}{R_i T_{gi}} & 0\\ \frac{1}{T_{ti}} & -\frac{1}{T_{ti}} & 0 & 0\\ 0 & \frac{1}{2H_i} & -\frac{D_i}{2H_i} & -\frac{1}{2H_i}\\ 0 & 0 & 2\pi\sum_{\substack{j=1\\ j\neq 1}}^{N} T_{ij} & 0 \end{bmatrix}\begin{bmatrix} \Delta P_{gi}\\ \Delta P_{mi}\\ \Delta f_i\\ \Delta P_{tie,i} \end{bmatrix} + \begin{bmatrix} 0 & 0\\ 0 & 0\\ -\frac{1}{2H_i} & 0\\ 0 & -2\pi \end{bmatrix}\begin{bmatrix} \Delta P_{Li}\\ \Delta V_i \end{bmatrix} + \begin{bmatrix} \frac{1}{T_{gi}}\\ 0\\ 0 \end{bmatrix}\Delta P_{ei}\\ y = ACE_i = [0\ 0\ B_i\ 1] \end{array}\right\} \tag{12}$$

$$\left\{\begin{array}{l} \begin{bmatrix} \Delta\dot{P}_{gi}\\ \Delta\dot{P}_{mi}\\ \Delta\dot{f}_i\\ \Delta\dot{P}_{tie,i}\\ \Delta\dot{i}_{qr,i}\\ \Delta\dot{w}_i \end{bmatrix} = \begin{bmatrix} -\frac{1}{T_{gi}} & 0 & -\frac{1}{R_i\cdot T_{gi}} & 0 & 0 & 0\\ \frac{1}{T_{ti}} & -\frac{1}{T_{ti}} & 0 & 0 & 0 & 0\\ 0 & \frac{1}{2H_i} & -\frac{D}{2H_i} & -\frac{1}{2H_i} & -\frac{X_3\cdot w_{opt}}{2H_i} & 0\\ 0 & 0 & 2\pi\sum_{\substack{j=1\\ j\neq 1}}^{N} T_{ij} & 0 & 0 & \\ 0 & 0 & 0 & 0 & -\frac{1}{T_1} & 0\\ 0 & 0 & 0 & 0 & -\frac{X_3}{2H_t} & 0 \end{bmatrix}\begin{bmatrix} \Delta P_{gi}\\ \Delta P_{mi}\\ \Delta f_i\\ \Delta P_{tie,i}\\ \Delta i_{qr,i}\\ \Delta w_i \end{bmatrix} + \begin{bmatrix} \frac{1}{T_{gi}} & 0\\ 0 & 0\\ 0 & 0\\ 0 & 0\\ 0 & \frac{X_2}{T_1}\\ 0 & 0 \end{bmatrix}\begin{bmatrix} \Delta P_{ci}\\ \Delta V_{qr} \end{bmatrix} + \begin{bmatrix} 0 & 0 & 0\\ 0 & 0 & 0\\ -\frac{1}{2H_i} & 0 & 0\\ 0 & -2\pi & 0\\ 0 & 0 & 0\\ 0 & 0 & \frac{1}{2H_t} \end{bmatrix}\begin{bmatrix} \Delta P_{Li}\\ \Delta V_i\\ \Delta T_m \end{bmatrix}\\ y = \begin{bmatrix} 0 & 0 & B_i & 1 & 0 & 0\\ 0 & 0 & 0 & 0 & 0 & 1 \end{bmatrix}\begin{bmatrix} \Delta P_g\\ \Delta P_m\\ \Delta f\\ \Delta P_{tie,i}\\ \Delta i_{qr}\\ \Delta w \end{bmatrix} \end{array}\right\} \tag{11}$$

Author Personal Copy

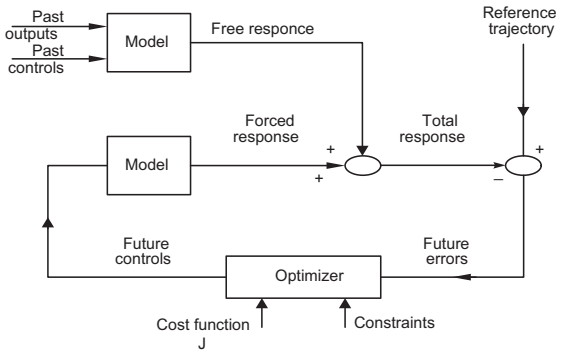

Fig. 3. A simple structure of the MPC controller.

4. Model predictive control

The MPC has proved to efficiently control a wide range of applications in industry such as chemical process, petrol industry, electromechanical systems and many other applications. The MPC scheme is based on an explicit use of a prediction model of the system response to obtain the control actions by minimizing an objective function. Optimization objectives include minimization of the difference between the predicted and reference response, and the control effort subjected to prescribed constraints. The effectiveness of the MPC is demonstrated to be equivalent to the optimal control. It displays its main strength in its computational expediency, real-time applications, intrinsic compensation for time delays, treatment of constraints, and potential for future extensions of the methodology. At each control interval, the first input in the optimal sequence is sent into the plant, and the entire calculation is repeated at subsequent control intervals. The purpose of taking new measurements at each time step is to compensate for unmeasured disturbances and model inaccuracy, both of which cause the system output to be different from the one predicted by the model [8,9].

Fig. 3 shows a simple structure of the MPC controller. An internal model is used to predict the future plant outputs based on the past and current values of the inputs and outputs and on the proposed optimal future control actions. The prediction has two main components: the free response which being expected behavior of the output assuming zero future control actions, and the forced response which being the additional component of the output response due to the candidate set of future controls. For a linear systems, the total prediction can be calculated by summing both of free and forced responses. The optimizer is used to calculate the best set of future control action by minimizing a cost function (J). The optimization is subject to constraints on both manipulated and controlled variables [10].

Table 2
Parameters and data of a practical single area power system.

D (pu/Hz)	H (pu s)	R (Hz/pu)	T_g (s)	T_t (s)
0.015	0.08335	3.00	0.08	0.4

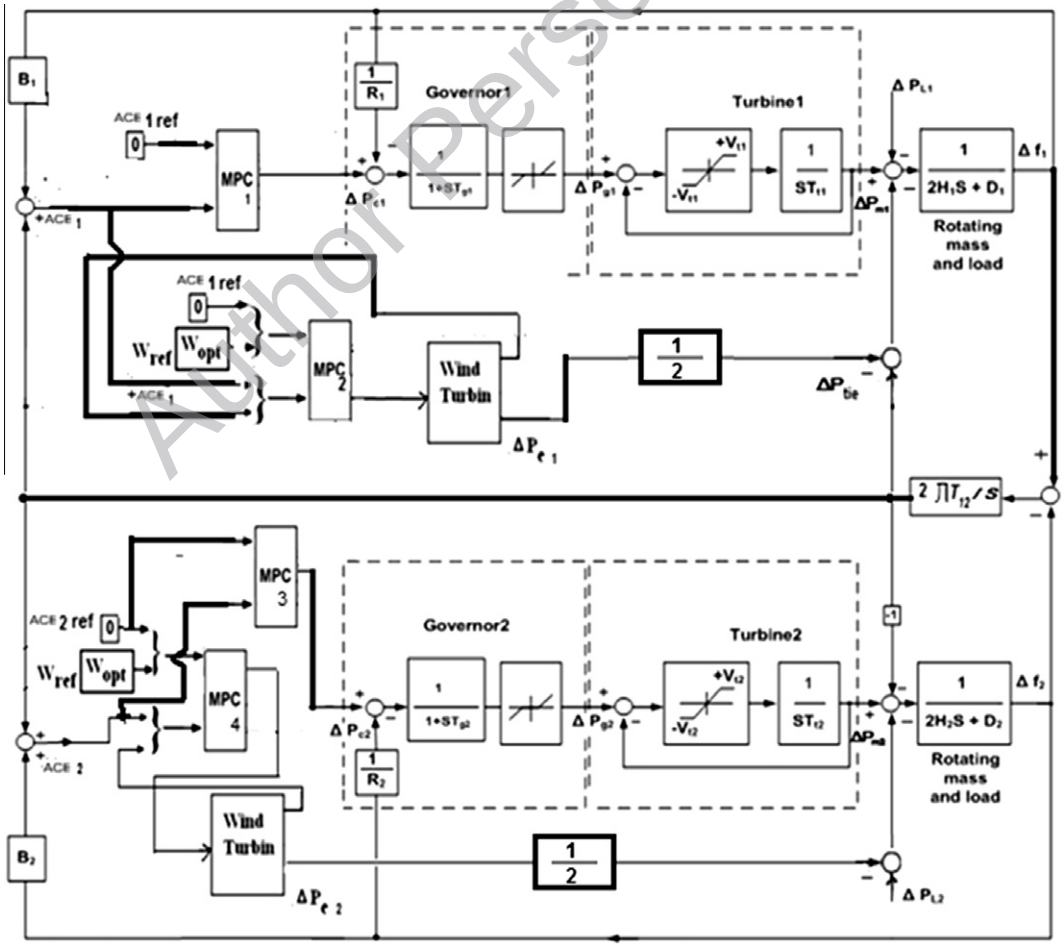

Fig. 4. The block diagram of a two area power system including the proposed MPC controller and WT.

Author Personal Copy

The general objective is to tighten the future output error to zero, with a minimum input effort. The cost function to be minimized is generally a weighted sum of square predicted errors and square future control values, e.g. in the Generalized Predictive Control (GPC):

$$J(N_1,N_2,N_u)=\sum_{j=N_1}^{N_2}\beta(j)[\hat{y}(k+j|k)-w(k+j)]^2+\sum_{j=1}^{N_u}\lambda(j)[u(k+j-1)]^2 \quad (13)$$

where N_1, N_2 are the lower and upper prediction horizons over the output, N_u is the control horizon, $\beta(j),\lambda(j)$ are weighting factors. The control horizon permits to decrease the number of calculated future control according to the relation: $\Delta u(k+j)$ for $J \geqslant N_u$. The $w(k+j)$ represents the reference trajectory over the future horizon N.

Constraints over the control signal, the outputs and the control signal changing can be added to the cost function as follows:

$$\begin{aligned} &u_{min} \leqslant u(k) \leqslant u_{max} \\ &\Delta u_{min} \leqslant \Delta u(k) \leqslant \Delta u_{max} \\ &y_{min} \leqslant y(k) \leqslant y_{max} \end{aligned} \quad (14)$$

Solution of Eq. (13) gives the optimal sequence of control signal over the horizon N while respecting the given constraints of Eq. (14).

The MPC have many advantages, in particularly it can pilot a big variety of process, being simple to apply in the case of multivariable system, can compensate the effect of pure delay by the prediction, inducing the anticipate effect in the closed loop, being a simple technique of control to be applied and also offer optimal solution while respecting the given constraints. On the other hand, this type of restructure required the knowledge of model for the system, and in the presence of constraints it becomes a relatively more complex regulator than a simple conventional controller such as a proportional integral differential (PID), and it takes more time for on-line calculations

5. System configuration

The block diagram of a simplified frequency response model for a two area power system with aggregated unit including the proposed MPC controller is shown in Fig. 4. Each area consists of the overall rotating mass and load and an aggregated generator unit including one nonlinear turbine with GRC, one governor with dead-band constraint [1], and aggregated wind turbine model (which consists of 200 wind turbine units of 2 MW rated VSWTs), as each local area controller can be designed independently. On the other hand, the frequency deviation and wind turbine rotational speed are used as feedback for the closed loop control system. Both of the reference and measured area control error ACE_i, ($ACE_{ref,i}$ = 0 HZ) and both of the reference and measured wind rotational speed ($w_{ref,i} = w_{opt}$) are fed to the model predictive controller $MPC_{i,2}$ of the wind turbine unit in order to obtain the signal $\Delta V_{qr,i}$ (q-axis component of the deviation of the rotor voltage, which fed to the wind turbine), and the second controller $MPC_{i,1}$ is fed by only by the reference and measured area control error ACE_i, ($ACE_{ref,i}$ = 0 HZ) in order to obtain the supplementary control action ΔP_{ci} which is added to the negative frequency feedback signal to give the signal which feeds the governor giving the governor valve position which supplies the turbine to give the mechanical power change ΔP_{mi} which is affected by the load change ΔP_{Li}, the tie-line power change $\Delta P_{tie,i}$ and the active power change of wind turbine ΔP_e (which multiplied by a gain equal to 0.5 to make a correlation

Table 3
Wind turbine parameters and operating point [14].

Operating point (mw)	Wind speed (m/s)	Rotational speed (m/s)	R_r (pu)	R_s (pu)	X_{lr} (pu)	X_{ls} (pu)	X_m (pu)	H_t (pu)
247	11	1.17	0.00552	0.00491	0.1	0.09273	3.9654	4.5

X_m is the magnetizing reactance, $(P_{wt})_{Base}$ = 400 MVA, $(w_r)_{Base}$ = 1.15 (rad/s).

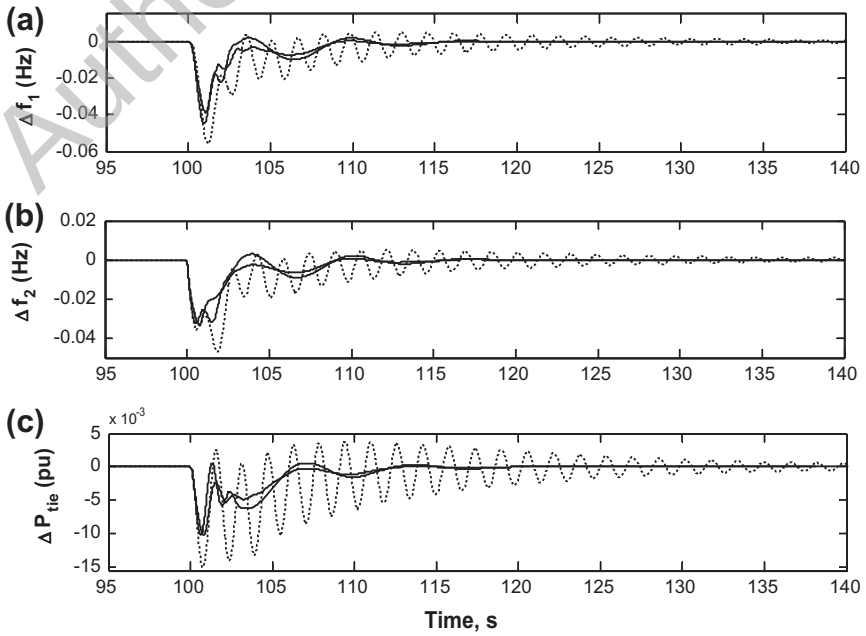

Fig. 5. Power system response for case1 of Scenario 1: with (MPC with WT participation) (bold and solid curve) and with (MPC without WT participation) (solid and thin curve) and conventional controller (dotted curve).

Author Personal Copy

between power system and wind turbine bases) giving the input of the rotating mass and load block to provide the actual frequency deviation Δf. In addition, the tie-line flow deviation is added to the frequency deviation in the supplementary feedback loop to give the area control error ACE_i.

6. Results and discussions

Computer simulations have been carried out in order to validate the effectiveness of the proposed scheme. The Matlab/Simulink software package has been used for this purpose. A practical multi area power system with the nominal parameters [1] listed in Table 2, is considered.

The simulation studies are carried out for the proposed controller with generation rate constraint (GRC) of 10% pu per minute. The maximum value of dead band for governor is specified as 0.05%. The parameters of the MPC controller are set as follows:

prediction horizon = 10,
control horizon = 2,
weights on manipulated variables = 0,
weights on manipulated variable rates = 0.1,
weights on the output signals = 1, and
sampling interval = 0.1 s.

Constraints are imposed over the control action, and frequency deviation are considered as follows :

Max. control action = 0.25 pu.
Min. control action = −0.25 pu.
Max. frequency deviation = 0.25 pu.

Author Personal Copy

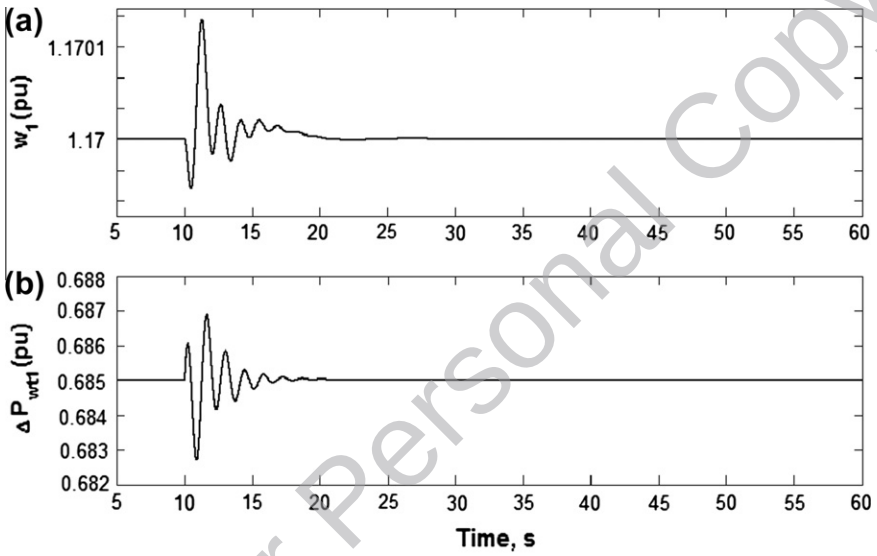

Fig. 6. Wind turbine responses in the first case, (a) rotational speed w, and (b) power change of wind turbine ΔP_{e1}.

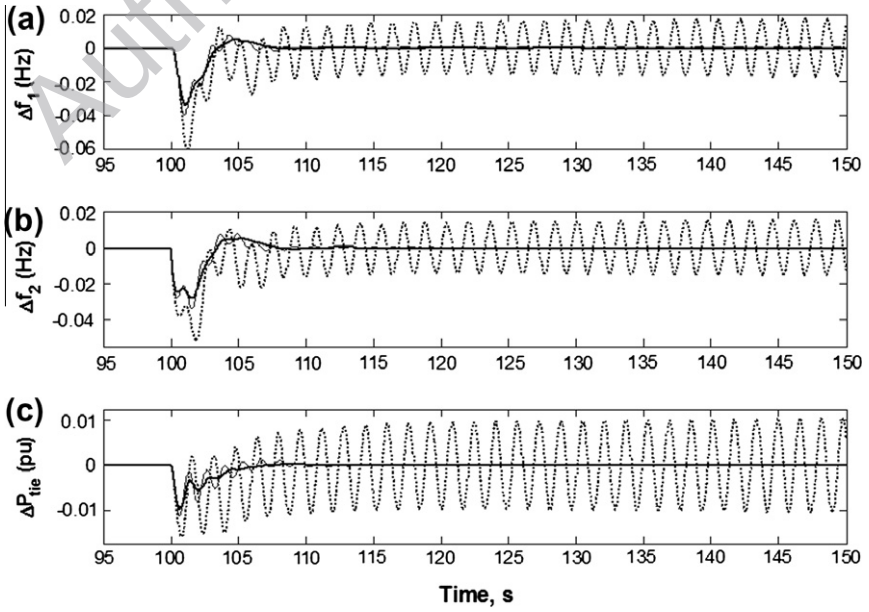

Fig. 7. Power system response forcase 2 of Scenario 1, with (MPC with WT participation) (thick and solid curve) and with (MPC without WT participation) (solid and thin curve) and conventional controller (dotted curve).

Min. frequency deviation = −0.25 pu.

The wind turbine used consists of 200 units of 2 MW rated variable speed wind turbine VSWTs, the wind turbine parameters and operating point are indicated in Table 3.

6.1. Scenario 1

6.1.1. Case 1

The system performance with the proposed MPC controllers in case of wind turbine participation at nominal parameters is tested and compared with the system performances with both MPC controllers without wind turbine participation using a conventional integrator ($K(s) = -0.3/s$) in the presence of a step load change (ΔP_L is assumed to be 0.02 pu at $t = 100$ s). Fig. 5 shows the simulation results of the MPC with WT participation, MPC without WT participation (as in [15]) and only conventional integrator systems. The results from the top to the bottom are: the frequency deviations for Area_1, the frequency deviations for Area_2, and the tie-line power change $\Delta P_{tie,i}$. It has been noticed that with the proposed MPC controller with the participation of WT, the system is more stable and fast compared to the system with conventional controller and merging the wind turbine leaded to the enhancement of the performance of the MPC controller. Fig. 6 shows both rotational speed (at the top) and power change of wind turbine (at the bottom). As shown in this figure, the change in the wind turbine electrical power can cooperate to enhance the overall system response performance.

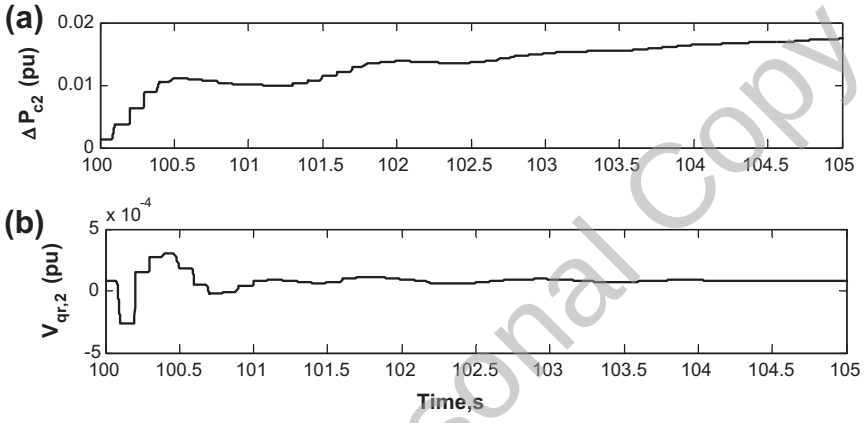

Fig. 8. System control signals: (a) output of MPC3, (b) output of MPC4.

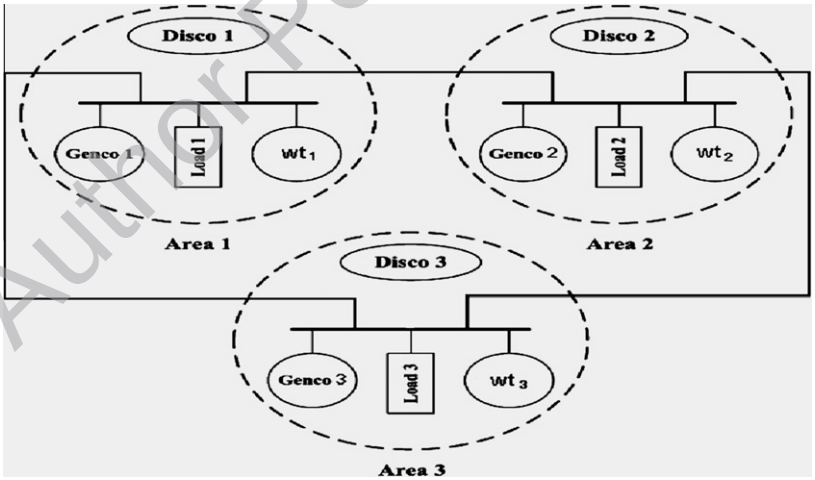

Fig. 9. Three-control area power system with wind turbines.

Table 4
Parameters and data of a practical three control area power system.

Area	$K(s)$	D (pu/Hz)	$2H$ (pu s)	R (Hz/pu)	T_g (s)	T_t (s)	T_{ij}
Area-1	−0.3/s	0.015	0.1667	3.00	0.08	0.40	$T_{12} = 0.20$ $T_{13} = 0.25$
Area-2	−0.2/s	0.016	0.2017	2.73	0.06	0.44	$T_{21} = 0.20$ $T_{23} = 0.15$
Area-3	−0.4/s	0.015	0.1247	2.82	0.07	0.3	$T_{31} = 0.25$ $T_{32} = 0.15$

$(P_e)_{Base}$ = 800 MVA.

Author Personal Copy

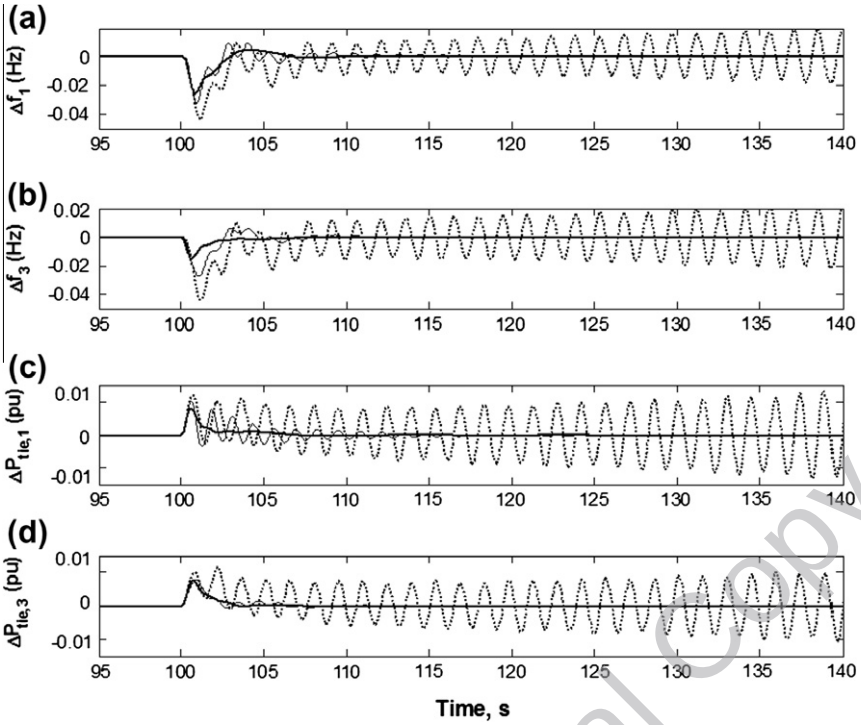

Fig. 10. Power system response to scenario B with MPC with participation of wind turbines (thick and solid curve), only MPC (solid and thin curve) controller, and conventional controller (dotted curve).

6.1.2. Case 2

The robustness of the proposed system against parameters uncertainty is validated. In this case, both of the governor and turbine time constants are increased to Tg1 = 0.105 s (≅31% change), Tt1 = 0.785 s (≅95% change), Tg2 = 0.105 s (≅66% change) and Tt2 = 0.6 s (≅38% change), respectively (this can happen in case of off line change of the practical turbine and governor, while the controller keeps the nominal values of these parts). Fig. 7 depicts the system response with MPC with WT participation, MPC without WT participation and only integrator in this case of study. The load change is assumed to be as described in the first case. It has been shown that, with the traditional controller, the system becomes unstable while with the MPC controller, the system response is more convenient. Also, the figure indicates that the presence of wind turbine leads to enhance the system performance with MPC controller, significantly. While Fig. 8 shows the control signals of the controllers MPC3 and MPC4 of Area 2.

6.2. Scenario 2

To illustrate the behavior of LFC system with the proposed decentralized MPC controller in the presence of wind turbine in a multi-area power system, consider three identical interconnected control areas as shown in Fig. 9. The simulation parameters [1] are given in Table 4, while the wind turbine parameters are the same for all areas and are listed in Table 3. The system is tested at a simultaneous 0.02-pu load step disturbance in control area-2 and against wide range of parameters uncertainty is validated. In this case, the governor and turbine time constants of each area are increased to Tg1 = 0.105 s (≅31% change), Tt1 = 0.785 s (≅95% change), Tg2 = 0.105 s (≅66% change) and Tt2 = 0.6 s (≅38% change), Tg3 = 0.15 s (≅100% change) and Tt3 = 0.7 s (≅100% change), respectively. Fig. 10 depicts the response of both the proposed MPC controllers in the presence and without the participation of the wind turbine (as in [15]) and that response of the classical integrator controller (with gains listed in Table 4) in the case of above uncertainty. The results from the top to the bottom are: frequency deviation in area-1, frequency deviation in area-3, tie-line power change in area-1, and tie-line power change in area-3. From the comparisons in Fig. 10, that even at this severe condition of uncertainties, system with MPC controllers keeps stable, and it is appeared that wind turbine affected positively on the system response.

7. Conclusions

This paper studies the merging of wind turbines in a multi area power system controlled by a robust load frequency control based on the model predictive control technique.

Digital simulations have been carried out in order to validate the effectiveness of the proposed scheme. The proposed controller has been tested for several mismatched parameters and load disturbance.

A performance comparison between the proposed MPC in the presence of wind turbine and MPC without wind turbine and conventional integral controllers is carried out. The simulation results demonstrate that the closed-loop system with MPC controller is robust against the parameter perturbation of the system and has desirable performance in comparison of classical integral control design in all of the performed test scenarios. Also, it was denoted that wind turbine has a positive impact on the total response of the system. For future work, to solve the problem of the complex optimization problem procedure required in MPC design, simulation results can be used to train a neural network to give the same robust response with ability of practical implementation.

Appendix A. A

Fig. 1 shows a simplified model of DFIG based wind turbine (WT) for frequency response, this model is investigated from the detailed model [17], which can be described As:

Voltage equations

Author's personal copy

$$V_{ds} = R_S i_{ds} - \psi_{qs} + \frac{1}{w_S}\frac{d}{dt}\psi_{ds} \quad (A.1)$$

$$V_{qs} = R_S i_{qs} - \psi_{ds} + \frac{1}{w_S}\frac{d}{dt}\psi_{qs} \quad (A.2)$$

$$V_{dr} = R_r i_{dr} - s\psi_{qs} + \frac{1}{w_S}\frac{d}{dt}\psi_{dr} \quad (A.3)$$

$$V_{qr} = R_r i_{qr} + s\psi_{dr} + \frac{1}{w_S}\frac{d}{dt}\psi_{qr} \quad (A.4)$$

Flux equations

$$\psi_{ds} = L_{ss} i_{ds} + L_m i_{dr} \quad (A.5)$$

$$\psi_{qs} = L_{ss} i_{qs} + L_m i_{qr} \quad (A.6)$$

$$\psi_{dr} = L_{rr} i_{dr} + L_m i_{ds} \quad (A.7)$$

$$\psi_{qr} = L_{rr} i_{qr} + L_m i_{qs} \quad (A.8)$$

where

$$L_{ss} = L_s + L_m$$

and

$$L_{rr} = L_r + L_m$$

Torque equation

$$T_e = \psi_{ds} \times i_{qs} - \psi_{qs} \times i_{ds} = \psi_{dr} \times i_{qr} - \psi_{qr} \times i_{dr} \quad (A.9)$$

Manipulating (A.1), (A.2), (A.3), (A.4), (A.5), (A.6), (A.7), (A.8) the following equations can be derived:

$$\dot{i_{dr}} = -\frac{w_S R_r}{L_{rr}} i_{dr} + s \times w_s \times i_{qr} + \frac{w_s}{L_{rr}} \times V_{dr} + s \times w_s \times \frac{L_m}{L_{rr}} \times i_{qs} - \frac{L_m}{L_{rr}} \times \dot{i_{ds}} \quad (A.10)$$

$$\dot{i_{qr}} = -\frac{w_S R_r}{L_{rr}} i_{qr} - s \times w_s \times i_{dr} + \frac{w_s}{L_{rr}} \times V_{qr} - s \times w_s \times \frac{L_m}{L_{rr}} \times i_{ds} - \frac{L_m}{L_{rr}} \times \dot{i_{qs}} \quad (A.11)$$

For vector control of the DFIG, the d-axis was chosen such that it coincides with the maximum of the stator flux, therefore, ψ_{ds} = 1 pu and ψ_{qs} = 1 pu. Substituting in (A.6), the following equation can be obtained:

$$i_{qs} = -\frac{L_m}{L_{SS}} i_{qr} \quad (A.12)$$

then Eq. (A.11) can be simplified and converted to S domain as:

$$S\left[1 - \frac{L_m^2}{L_{SS} L_{rr}}\right] i_{qr} = -\frac{w_S R_r}{L_{rr}} i_{qr} + \frac{w_s}{L_{rr}} V_{dr} \quad (A.13)$$

and

$$i_{qr} = \frac{1}{R_r} \times \frac{1}{[1 + ST_1]} V_{qr} \quad (A.14)$$

substituting, ψ_{ds} = 1 pu and ψ_{qs} = 1 pu in (A.9) and the using (A.12), the following equation can be obtained for the electromagnetic torque:

$$T_e = i_{qs} = -\frac{L_m}{L_{SS}} i_{qr} \quad (A.15)$$

While the mechanical equation can described as:

$$p_e = T_e w_r \quad (A.16)$$

References

[1] Bevrani H. Robust power system control. New York: Springer; 2009.
[2] Talaq J, Al-Basri F. Adaptive fuzzy gain scheduling for load frequency control. IEEE Trans Power Syst 1999;14(1):145–50.
[3] HO Jae Lee, Jin Bae Park, Young Hoon Joo. Robust LFC for Uncertain nonlinear power systems: a fuzzy logic approach. Inform Sci 2006;176:3520–37.
[4] Alireza Yazdizadeh, Mohammad Hossein Ramezani, Ehsan Hamedrahmat. Decentralized load frequency control using a new robust optimal MISO PID controller. Electr Power Energy Sys 2012;35:57–65.
[5] cam E, Kocaarslan I. Load frequency control in two area power systems using fuzzy logic controller. Energy Convers Manage 2005;46:233–43.
[6] Birch AP, Sapeluk AT, Ozveren CS. An enhanced neural network load frequency control technique. ASCE J 2005;5(II) [Control 94, 21–24 March 1994, Conference Publication No. 389, IEE 1994].
[7] Reza Farhangi, Mehrdad Boroushaki, Seyed Hamid Hosseini. Load–frequency control of interconnected power system using emotional learning-based intelligent controller. Electr Power Energy Sys 2012;36:76–83.
[8] Thomas J, Dumur D, Buisson J, Gueguen H. Model predictive control for hybrid systems under a state partition based MLD approach (SPMLD). In: International conference on informatics in control, automation and robotics ICINCO'04, vol. 3, Setúbal; 2004. p. 78–85.
[9] Richalet J, Rault A, Testud JL, Japon J. Model predictive heuristic control. application to industrial processes. Automatica 1978;14(5):413–28.
[10] De Silva Clarence W. Mechatronic systems : devices, design, control, operation and monitoring. Taylor and Francis Group, LLC; 2008.
[11] Mullane A, O'Malley M. The inertial response of induction-machine-based wind turbines. IEEE Trans Power Sys 2005;20(3):1496–503.
[12] Holdsworth L, Ekanayake JB, Jenkins N. Power system frequency response from fixed speed and doubly fed induction generator-based wind turbines. Wind Energy 2004;7:21–35.
[13] Mohamed TH, Bevrani H, Hassan AA, Hiyama T. Model predictive based load frequency control design. In: 16th international conference of electrical engineering, Busan, Korea; July 2010.
[14] Morel J, Bevrani H, Ishii T, Hiyama T. A robust control approach for primary frequency regulation through variable speed wind turbines. IEEJ Trans PE 2010;130(11):1002–9.
[15] Mohamed TH, Bevrani H, Hassan AA, Hiyama T. Decentralized model predictive based load frequency control in an interconnected power system. Energy Convers Manage 2011;52:1208–41.
[16] Yaser Soliman Qudaih, Michael Bernard, Yasunori Mitani, Mohamed TH. Model predictive based load frequency control design in the presence of DFIG wind turbine. In: Proceeding of the 2nd international conference on electric power and energy conversion systems (EPECS'11), Sharjah, UAE; November 15–17, 2011.
[17] Ekanayake JB, Jenkins N, Strbac G. Frequency response from wind turbines. Wind Eng 2008;32(6):573–86.

Author Personal Copy